Slip and Flow in Soft Particle Pastes

Steven P. Meeker,[1] Roger T. Bonnecaze,[2] and Michel Cloitre[1,*]

[1]*Laboratoire Matière Molle et Chimie (UMR 167, CNRS/ESPCI), ESPCI, 10 rue Vauquelin, 75321 Paris Cedex, France*

[2]*Department of Chemical Engineering and Texas Materials Institute, The University of Texas at Austin, Austin, Texas 78712, USA*

(Received 29 July 2003; published 11 May 2004)

Concentrated dispersions of soft particles are shown to exhibit a generic slip behavior near smooth surfaces. Slip results from a balance between osmotic forces and noncontact elastohydrodynamic interaction between the squeezed particles and the wall. A model is presented that predicts the slip properties and provides insight into the behavior of the bulk paste.

DOI: 10.1103/PhysRevLett.92.198302 PACS numbers: 82.70.–y, 83.50.Rp, 83.60.La

Concentrated dispersions such as colloidal pastes, emulsions, and granular suspensions display both solidlike and fluidlike flow properties [1]. Their close-packed, amorphous structures lie at the heart of this behavior. The particles are jammed [2] and can only flow past one another appreciably if a large enough stress, greater than the ''yield'' stress, is applied. This unique property is exploited to form high performance materials in many engineering processes, such as film coating, screen printing, and ceramic extrusions. However, the motion of a concentrated dispersion depends not only on the bulk flow properties but also upon the nature of the confining surfaces. Put simply, a paste often prefers to ''slide'' rather than flow if the surfaces are suitably smooth. This can have a dramatic effect on the rheology and the processing of yield stress materials.

Wall effects in dispersion flows have often been described in terms of an apparent slip, which arises from a depletion of particles at the wall [3–9]. The presence of slip is generally inferred from the macroscopic rheological behavior, and several techniques have been developed to subtract slip effects and extract bulk rheology [3,5]. Only a few studies have tried to correlate the rheology with direct flow visualizations [4,6,8,9]. Very recently, another line of thought has emerged, which considers that the flow of concentrated dispersions should be intrinsically heterogeneous as a consequence of their particular glasslike dynamics [10–12]. In this context, several important questions remain open. What are the microscopic mechanisms at work when concentrated dispersions flow along surfaces? How are wall phenomena coupled to the bulk rheology? Is there any underlying universality?

In this Letter we answer these questions for the case of soft particle pastes. We probe simultaneously the nonlinear rheology and the local velocity profiles for different wall properties. When sheared between rough walls, pastes flow homogeneously over the whole range of shear rates investigated. When sheared between smooth walls, they exhibit wall slip. At high stresses, slip occurs but is negligible. Just above the yield stress σ_y the deformation results from a combination of paste flow and apparent slip. The slip velocity V has a constant value $V^* \sim G_0 R/\eta_S$, where G_0 is the low-frequency plateau storage modulus, η_S is the solvent viscosity, and R is the particle radius. Below σ_y the slip velocity V varies according to $V/V^* \sim (\sigma/\sigma_y)^2$. These properties are observed for different systems and over a wide range of experimental parameters, indicating a remarkable universality. A model, based on microelastohydrodynamic lubrication between squeezed particles and the wall, explains these results.

In this study we investigate microgel pastes and emulsions. In microgel pastes, each particle comprises a cross-linked polymer network of acrylate chains bearing ionized methacrylic acid groups, which is swollen by a solvent [13]. The solvents are water and water/glycerol mixtures. Two batches of microgels with cross-link density $N_x = 140$ and 28 are studied, N_x being the average number of monomers between cross-links. In dilute suspensions the particles have a spherical shape with a hydrodynamic radius R ($R = 220$ nm for $N_x = 140$ and $R = 125$ nm for $N_x = 28$). Above the concentration C_m the microgels pack into concentrated pastes with solidlike properties ($C_m = 0.0085$ g/g for $N_x = 140$ and $C_m = 0.038$ g/g for $N_x = 28$). The emulsions are concentrated dispersions of silicon oil (viscosity 0.5 Pa s) in water, stabilized by the surfactant Triton X-100 ($<10^{-2}$ g/g) [14]. The size distribution is moderately polydisperse, with a mean droplet radius $R \cong 1.5 \pm 1$ μm. The emulsions exhibit solidlike behavior above a volume fraction $\phi = 0.70$.

The macroscopic rheology has been measured using a stress-controlled rheometer (Haake RS 150) with cone and plate geometries (35 and 60 mm diameter, angle 2°). Rough geometries are obtained from the manufacturer (roughness ~ 5 μm) or prepared by sticking waterproof sandpaper on the shearing surfaces (roughness ~ 30 μm). Reproducible smooth geometries are obtained by covering the shearing surfaces with a polymer film. Quantitatively similar measurements are obtained with other smooth surfaces such as glass or metallic plates, indicating that the wetting properties of the substrate play no significant role in the phenomena reported below. Samples are sealed in a water-saturated environment to

 © 2004 The American Physical Society

minimize evaporation. A preshear stress, resulting in high shear rates ($\sim$1000 s^{-1} for the microgel pastes and $\sim$100 s^{-1} for the emulsions), is applied to the sample for 60 s prior to each measurement. The stress is then quenched to lower σ value and the steady-state apparent shear rate $\dot{\gamma}_{app}$ measured. Simultaneously, we have measured the flow profiles using video microscopy for typical microgel pastes. The pastes, which are translucent, are seeded at very low concentrations ($\cong 5 \times 10^{-4}$ g/g) with glass spheres (diameter ~ 10 μm) that reflect light when illuminated. They are observed from the side using a CCD camera equipped with a high magnification zoom lens. Local velocities are obtained by measuring the displacement of the tracers during time. By placing a transparent film at the sample periphery, we are able to focus the observation plane up to 6 mm into the bulk. All the measurements reported in the following are made at the fixed radial position $r = (0.79 \pm 0.02) r_{max}$, r_{max} being the cone and plate radius. We have checked carefully that the measurements are not influenced by edge effects.

Figure 1 shows the flow curves of a microgel paste and an emulsion measured with rough and smooth geometries. When sheared using rough surfaces, both systems display the nonlinear rheology of a yield stress fluid, well described by the Herschel-Bulkley equation [1]: $\sigma = \sigma_y + a\dot{\gamma}^n$. The yield stress σ_y is proportional to the elastic shear modulus G_0: $\sigma_y = G_0 \gamma_y$ with the yield strain $\gamma_y = 0.06$. The flow curves of the microgel paste and the emulsion are nearly superimposed, reflecting the same macroscopic bulk flow properties. This flow behavior is dramatically changed when the surfaces are smooth. The measured shear rate no longer vanishes at the yield stress σ_y and apparent flow is detected for stresses well below σ_y. At very low stresses the flow curves exhibit an apparent yield stress σ_y'. The flow curves measured for the microgel paste and the emulsion are very similar in shape, and simply map onto each other by rescaling the shear rate. Some of the features depicted in Fig. 1 have already been observed [4,7–9]. The interesting result here is that different yield stress materials exhibit a generic behavior, suggesting some underlying universality.

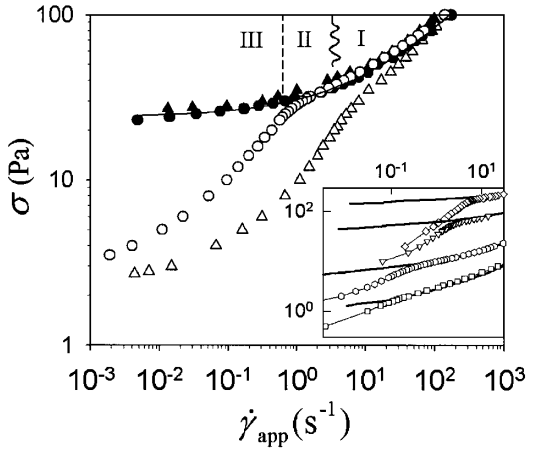

FIG. 1. Generic slip flow curves (smooth surfaces) for a microgel paste (○) ($C = 0.02$ g/g, $N_x = 140$) and an emulsion (△) ($\phi \cong 0.77$), with the same bulk rheology (rough surfaces; ●, ▲). The solid line is the Herschel-Bulkley fit to the microgel data ($\sigma_y = 24 \pm 2$ Pa, $n = 0.48$, $a = 6.7$). Regimes I–III refer to microgel slip behavior. The inset shows flow curves with (○) and without (solid line) slip for various microgel pastes (from bottom to top: $G_0 = 29$, 128, 1200, and 2900 Pa).

Figure 2 shows the velocity profiles for microgel pastes. When sheared with rough surfaces, the pastes flow homogeneously in the whole range of stresses and shear rates accessible by our experimental setup ($2 \times 10^{-3} \leq \dot{\gamma} \leq 3$ s^{-1}) [Fig. 2(a)]. There is no evidence of shear banding, fracture, or wall slip. When the shearing surfaces are smooth, the velocity profiles still vary linearly [Figs. 2(b)–2(d)] but, at low stresses, they extrapolate to the cone and plate velocities not at the surfaces but far beyond [Figs. 2(c) and 2(d)]. This is the signature of wall slip. The slip layer is not resolvable in our setup, indicating that its thickness is smaller than 50 μm.

We identify three regimes of slip. Regime I is observed at high stresses (e.g., $\sigma/\sigma_y \geq 1.5$ for the microgel paste), where slip is negligible compared to the bulk flow [Fig. 2(b)]. The macroscopic rheology does not depend on the wall roughness. Regime II is observed just above the yield stress ($1 < \sigma/\sigma_y < 1.5$), where wall slip becomes significant and the total deformation results from a combination of bulk flow and slip [Fig. 2(c)]. Now, there is a clear influence of slip on the rheology. Regime III is observed at and below the yield stress ($\sigma/\sigma_y \leq 1$). The motion is due entirely to the slipping of the paste [Fig. 2(d)]. The rheological measurements

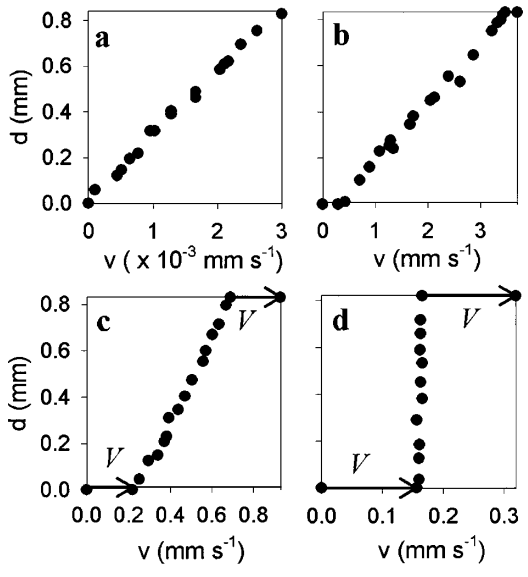

FIG. 2. Microgel paste flow profiles ($C = 0.02$ g/g, $N_x = 140$). Rough surfaces: $\sigma/\sigma_y = 1.05 \pm 0.1$ (a). Smooth surfaces: $\sigma/\sigma_y = 1.7 \pm 0.1$ (b), 1.3 ± 0.1 (c), and 0.9 ± 0.1 (d).

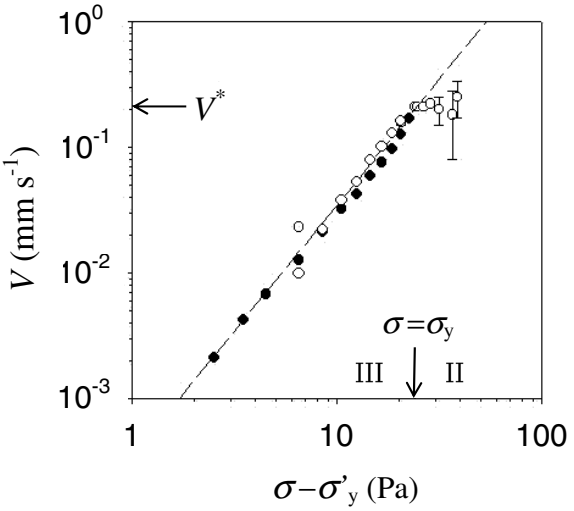

FIG. 3. The slip velocity V versus the excess stress $\sigma - \sigma'_y$ measured from visualization (○) and from rheology (●) (C = 0.02 g/g, $N_x = 140$; $\sigma'_y = 3.5$ Pa).

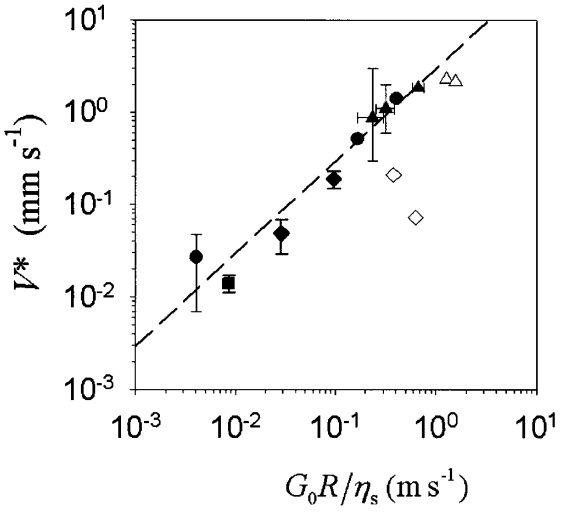

FIG. 4. V^* measured from rheology for microgel pastes: $N_x = 140$, $\eta_S = 0.9$ mPa s, $C = 0.015$ g/g (◆), 0.04 g/g, 0.06 g/g (◇); $N_x = 28$, $\eta_S = 0.9$ mPa s, $C = 0.045$ g/g, 0.055 g/g, 0.065 g/g (●); $N_x = 140$, $\eta_S = 9$ mPa s, $C = 0.02$ g/g (■); and emulsions: $\phi = 0.71$, 0.75, 0.77 (▲). 0.86, 0.93 (△). Scaling is obeyed for solid symbols.

probe the friction between the solidlike paste and the shearing surfaces.

Figure 3 shows the dependence of the slip velocity V on the excess stress $\sigma - \sigma'_y$. In regime III, the slip velocity decreases with the applied stress. The data are well represented by $V/V^* = [(\sigma - \sigma'_y)/(\sigma_y - \sigma'_y)]^2$, which reduces to $V/V^* \sim (\sigma/\sigma_y)^2$ since $\sigma'_y \ll \sigma_y$. This quadratic form agrees with previous results for emulsions [8]. In this regime, V can be determined directly from the rheological data by noting that it is simply half the relative velocity of the shearing surfaces. In regime II, the slip velocity remains equal to a plateau value V^*. At the onset of total slip ($\sigma = \sigma_y$) the characteristic slip velocity V^* is found to be simply half the cone edge velocity. The onset of total slip shifts to higher shear rates, i.e., V^* increases when the particle size R or the elastic modulus G_0 is increased (Fig. 1 and inset). Conversely V^* decreases when the solvent viscosity is increased. Interestingly, Fig. 4 shows that V^* is of the form $V^* \sim G_0R/\eta_S$ for all but the most concentrated samples.

To understand these results, we propose the following mechanism based on microelastohydrodynamic lubrication. In a paste, the particles are compressed and develop flat facets at the bounding surfaces. During motion, a lubricated layer of solvent can be maintained between the particles and the smooth surfaces. Indeed the flow in the fluid layer deforms the flattened particles asymmetrically. This results in a large pressure field, which creates a lift force pushing the particles away from the moving surfaces [15–17]. The balance between the lift force and the osmotic forces determines the thickness of the lubricated layer and ultimately the viscous drag between the particles and the surface. When the surface is rough, the lubricated film does not form and the no-slip situation is recovered. Elastohydrodynamic slip in soft particle pastes can be formalized as follows.

Figure 5 shows a microgel particle of radius R and elastic modulus G_P, against a wall. *At rest*, the particle is compressed by a distance h_0 and develops a facet of radius r_0 under pressure p_0 with the wall. Treating the facet as a Hertzian contact [18], we have $r_0 \sim R\xi_0^{1/2}$ and $p_0 \sim G_P\xi_0^{1/2}$, where $\xi_0 = h_0/R$. ξ_0 is obtained from the balance between the normal stress on a particle, $p_0(r_0/R)^2 \sim G_P\xi_0^{3/2}$, and the osmotic pressure of the paste. Assuming that the latter is proportional to the shear modulus G_0 [19], we find $\xi_0 \sim (G_0/G_P)^{2/3}$. *When the wall moves at velocity* V, the facet is separated from the wall by a lubricated layer of thickness δ. The pressure p in the layer is given by the lubrication equation [20]

$$\nabla \cdot [\delta^3(x, y)\nabla p(x, y)] = -6\eta_S V[\partial\delta(x, y)/\partial x]; \quad (1)$$

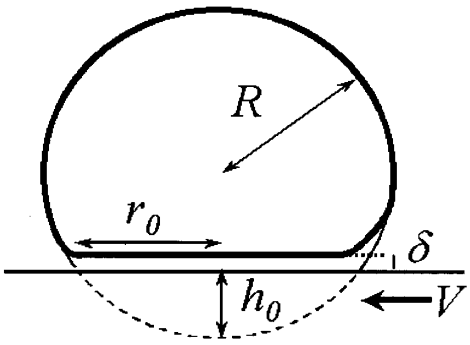

FIG. 5. Schematic of an elastohydrodynamically lubricated soft particle squeezed against a translating wall.

x and y are the Cartesian coordinates and ∇ is the two-dimensional gradient operator. Physically, the pressure p in the film must support the total deformation of the sphere, $\delta + h_0$. Expanding the previous expression of the pressure for Hertzian contacts, we find that $p = p_0 + O(\delta/h_0)$. For $\delta \ll h_0$, the variation of the pressure with velocity is negligible and to leading order $p \cong p_0$. Equation 1 scales as $\delta^3 p_0/r_0^2 \sim \eta_S V\delta/r_0$, from which $\delta \sim (\eta_S VR/G_P)^{1/2}$. δ increases with V as a consequence of $p \cong p_0$. The square-root dependence of δ on V has been observed experimentally with macroscopic rubber beads [21]. For a typical experiment ($\eta_S = 1$ mPa s, $R = 220$ nm, $G_P = 10^4$ Pa, $G_0 = 400$ Pa, $V = V^* = 0.2$ mm/s), we estimate $\delta \cong 2$ nm and $h_0 \cong 22$ nm. The assumption $\delta \ll h_0$ is well satisfied.

The macroscopic quantities δ and V can be expressed in terms of the particle-wall interactions. Let $F_d \sim \eta_S V r_0^2/\delta$ be the viscous drag on a particle. The average shear stress is then $\sigma \sim F_d/R^2$, and

$$\sigma \sim (\eta_S V/R)^{1/2}(G_0^4/G_P)^{1/6} \sim (\eta_S V G_0/R)^{1/2} f(C)^{1/6}. \tag{2}$$

The third term follows from the fact that the shear modulus of the paste can be expressed as [19,22] $G_0 = G_P f(C)$. The dependence of σ on concentration is weak and is neglected in the following. We find the characteristic slip velocity V^* by equating σ to the yield stress $\sigma_y \sim G_0\gamma_y$. The slip velocity V follows by inserting V^* into Eq. (2):

$$V^* \sim (G_0 R/\eta_S), \qquad V/V^* \sim (\sigma/\sigma_y)^2. \tag{3}$$

This analysis is valid for elastic particles such as microgels. An interesting issue is to determine whether it applies to emulsions with interfacial elasticity. A recent study of the compression of emulsion droplets is particularly useful in this context [23]. It has been shown that the interaction between compressed droplets is anharmonic and that the energy per facet is well described by $\varepsilon \sim \sigma_i \xi_0^\alpha R^2$, which yields a force of compression, $F_n \sim \sigma_i \xi_0^{\alpha-1} R^2$, where σ_i is the interfacial tension. The exponent α varies from 2.1 to 2.6 depending on the average coordination number. From the shape of a droplet compressed between two surfaces, it is also easy to show that the facet size varies as $r_0 \sim R\xi_0^\beta$ with $\beta \cong 0.6$. The contact pressure for the compressed droplet is then $p_0 \sim (\sigma_i/R)\xi_0^{\alpha-2\beta-1}$. These expressions of p_0 and r_0 are quite similar to their counterparts for microgels ($\sigma_i/R = G_P$). The above treatment of elastohydrodynamic slip can then be reworked for emulsions. We find that the shear stress is, in general, $\sigma \sim (\eta_S V G_0/R)^{1/2} f(C)^{\beta/2(\alpha-1)}$. The difference in the values of α and β between microgels and emulsions affects only the concentration dependence, but not the scaling with slip velocity and paste properties. Again the dependence on concentration is weak leaving results (3) unchanged.

These expressions reproduce the experimental behavior of microgel pastes and emulsions in the region of total slip. The nonscaling behavior of the most concentrated pastes and emulsions may arise from the divergence of osmotic pressure as $\phi \to 1$ [19], resulting in V and V^* values smaller than predicted by the model. We think that this slip mechanism based on elastohydrodynamic lubrication should apply to many concentrated dispersions of soft particles. Moreover, since jammed particles must "slip" past one another in order to move, similar mechanisms are likely to occur in the bulk of the material.

We thank Fabrice Monti for help in the experiments and Ludwik Leibler for stimulating discussions. S. P. M. was funded by a Marie Curie Host Fellowship. R. T. B. gratefully acknowledges the CNRS for supporting a sabbatical visit to the Laboratoire Matière Molle et Chimie where this work was done and the intellectually stimulating environment and hospitality provided by Ludwik Leibler and the members of the laboratory.

*Corresponding author.
Electronic address: michel.cloitre@espci.fr

[1] H. A. Barnes, J. Non-Newtonian Fluid Mech. **81**, 133 (1999).
[2] A. Liu and S. R. Nagel, Nature (London) **396**, 21 (1998); V. Trappe *et al.*, Nature (London) **411**, 772 (2001).
[3] M. Mooney, J. Rheol. **2**, 210 (1931).
[4] H. M. Princen, J. Colloid Interface Sci. **105**, 150 (1985).
[5] A. Yoshimura and R. K. Prud'homme, J. Rheol. **32**, 53 (1988).
[6] B. K. Aral and D. M. Kalyon, J. Rheol. **38**, 957 (1994).
[7] H. A. Barnes, J. Non-Newtonian Fluid Mech. **56**, 221 (1995).
[8] J. B. Salmon *et al.*, Eur. Phys. J. E **10**, 209 (2003).
[9] V. Bertola *et al.*, J. Rheol. **47**, 1211 (2003).
[10] P. Coussot *et al.*, Phys. Rev. Lett. **88**, 218301 (2002); J. S. Raynaud *et al.*, J. Rheol. **46**, 709 (2002).
[11] G. Picard *et al.*, Phys. Rev. E **66**, 051501 (2002).
[12] F. Varnik *et al.*, Phys. Rev. Lett. **90**, 095702 (2003).
[13] R. Borrega *et al.*, Europhys. Lett. **47**, 729 (1999).
[14] T. G. Mason and J. Bibette, Langmuir **13**, 4600 (1997).
[15] K. Sekimoto and L. Leibler, Europhys. Lett. **23**, 113 (1993).
[16] F. Lequeux, D. Grosshans, and R. Hocquart, Polym. Adv. Technol. **3**, 33 (1992).
[17] I. Cantat and C. Misbah, Phys. Rev. Lett. **83**, 880 (1999).
[18] K. L. Johnson, *Contact Mechanics* (Cambridge University, Cambridge, 1985), pp. 84–106.
[19] T. G. Mason, J. Bibette, and D. A. Weitz, Phys. Rev. Lett. **75**, 2051 (1995).
[20] W. M. Deen, *Analysis of Transport Phenomena* (Oxford University, New York, 1998), pp. 270–281.
[21] A. Martin *et al.*, Phys. Rev. E **65**, 031605 (2003).
[22] M. Cloitre *et al.*, C.R. Physique **4**, 221 (2003).
[23] M.-D. Lacasse *et al.*, Phys. Rev. Lett. **76**, 3448 (1996); M.-D. Lacasse, G. S. Crest, and D. Levine, Phys. Rev. E **54**, 5436 (1996).